Polymer Tubes with Longitudinal Composition Gradient by Face-to-Face Wetting†

Olaf Kriha,‡ Petra Göring,*,§ Marc Milbradt,§ Seema Agarwal,‡ Martin Steinhart,△ Ralf Wehrspohn,§ Joachim H. Wendorff,‡ and Andreas Greiner‡

Scientific Center of Materials Science, Department of Chemistry, Philipps-Universität Marburg, Hans-Meerwein-Strasse, D-35032 Marburg, Germany, Department of Physics, Martin-Luther-University Halle-Wittenberg, Heinrich Damerow-Strasse 4, D-06120 Halle, Germany, and Max Planck Institute of Microstructure Physics, Weinberg 2, D-06120 Halle, Germany

Received July 30, 2007. Revised Manuscript Received November 12, 2007

Nanoporous and macroporous templates were simultaneously infiltrated from both of their opposite surfaces using model polymers labeled with fluorescent probes or bearing probe molecules detectable by energy-dispersive X-ray spectroscopy by precursor wetting. Face-to-face wetting with polymeric solutions resulted in partial mixing of both components, leading to tubular nanostructures characterized by a longitudinal composition gradient. Mixing of the components infiltrated from the opposite surfaces could be prevented by face-to-face wetting with polymeric melts, leading to the formation of tubular components predominantly consisting of the pure components that were separated by sharp interfaces.

Introduction

The synthesis of one-dimensional nanostructures by means of nanoporous molds is a well-established approach that allows virtually any material to be formed into one-dimensional nanostructures.[1–4] Wetting porous templates such as porous alumina or macroporous silicon[5–7] with polymer melts or polymeric solutions is a simple and versatile method for the preparation of one-dimensional nanostructures consisting of a broad range of polymeric materials with diameters ranging from a few tens of nanometers to micrometers. Two different mechanisms guiding the filling of porous materials with polymeric liquids have been identified. If the polymer molecules are mobile enough to be removed from the bulk, mesoscopic polymeric precursor films with a thickness on the same order of magnitude as the radii of gyration of their constituents form within seconds on the pore walls. Spreading on pore walls differs from spreading on smooth substrates[8–10] in that in the former case, a liquid reservoir with an "infinite" volume on top of the porous template is in contact with a finite surface to be wetted, whereas in the latter case, the liquid reservoir has a finite volume and the substrate to be wetted an infinite surface. If the pore diameter exceeds twice the thickness of the wetting layer, which is determined by entropic relaxation of the polymer chains and the disjoining pressure,[11] tubular structures can easily be conserved by solidification of the infiltrated polymer.[12,13] If the mobility of the polymer chains is sufficiently reduced by heating the polymers only slightly above their glass-transition temperature[14] or in liquid, microphase-separated block copolymers,[15] single chains can no longer be removed from the liquid bulk reservoir. Instead, a solid thread of the polymeric liquid preceded by a meniscus moves in the pores driven by capillary forces. The length of the pore segments filled with polymer is proportional to the square root of the infiltration time[15,16] and can conveniently be adjusted by quenching the samples. Tentative results indicate that a transition from precursor wetting to capillary wetting also occurs if the pore walls are modified with nonpolar silane coupling agents.[17] A multitude of polymers can be formed into one-dimensional nanostructures by both precursor wetting and capillary wetting.[18–22]

† Part of the "Templated Materials Special Issue."

* Corresponding author. Telephone: 49 345 5528 515. Fax: 49 345 5527 391. E-mail: petra.goering@physik.uni-halle.de.

‡ Philipps-Universität Marburg.

§ Martin-Luther-University Halle-Wittenberg.

△ Max Planck Institute of Microstructure Physics.

(1) Penner, R. M.; Martin, C. R. *J. Electrochem. Soc.* **1986**, *133*, 2206.
(2) Martin, C. R.; Vandyke, L. S.; Cai, Z. H; Liang, W. B *J. Am. Chem. Soc.* **1990**, *112*, 8976.
(3) Martin, C. R. *Science* **1994**, *266*, 1961.
(4) Cepak, V. M.; Martin, C. R. *Chem. Mater.* **1999**, *11*, 1363.
(5) Lehmann, V. *J. Electrochem. Soc.* **1993**, *140*, 2836.
(6) Lehmann, V. *Electrochemistry of Silicon*; Wiley-VCH: Weinheim, Germany, 2002.
(7) Birner, A.; Wehrspohn, R. B.; Gösele, U.; Busch, K. *Adv. Mater.* **2001**, *13* (6), 377.
(8) de Gennes, P. G. *Rev. Mod. Phys.* **1985**, *57*, 827.
(9) Léger, L.; Joanny, J. F. *Rep. Prog. Phys.* **1992**, *55*, 431.
(10) Ausseré, D.; Picard, A. M.; Léger, C. *Phys. Rev. Lett.* **1986**, *57*, 2671.
(11) Derjaguin, B. V.; Churaev, N. V. *J. Colloid Interface Sci.* **1974**, *49*, 249.
(12) Steinhart, M.; Wendorff, J. H.; Greiner, A.; Wehrspohn, R. B.; Nielsch, K.; Schilling, J.; Choi, J.; Gösele, U. *Science* **2002**, *296*, 1997.
(13) Steinhart, M.; Wehrspohn, R. B.; Gösele, U.; Wendorff, J. H. *Angew. Chem., Int. Ed.* **2004**, *43*, 1334.
(14) Zhang, M.; Dobriyal, P.; Chen, J.-T.; Russell, T. P.; Olmo, J.; Merry, A. *Nano Lett.* **2006**, *5*, 1075.
(15) Xiang, H. Q.; Shin, K.; Kim, T.; Moon, S. I.; McCarthy, T. J.; Russell, T. P. *Macromolecules* **2004**, *37*, 5660.
(16) Kim, E.; Xia, Y.; Whitesides, G. M. *Nature* **1995**, *376*, 581.
(17) Grimm, S.; Schwirn, K.; Göring, P.; Knoll, H.; Miclea, P. T.; Greiner, A.; Wendorff, J. H.; Wehrspohn, R. B.; Gösele, U.; Steinhart, M. *Small* **2007**, *3*, 993.
(18) Steinhart, M.; Wendorff, J. H.; Wehrspohn, R. B. *ChemPhysChem.* **2003**, *4*, 1171.
(19) Steinhart, M.; Jia, Z.; Schaper, A.; Wehrspohn, R. B.; Gösele, U.; Wendorff, J. H. *Adv. Mater.* **2003**, *15*, 706.
(20) Steinhart, M.; Zimmermann, S.; Göring, P.; Schaper, A. K.; Gösele, U.; Weder, C.; Wendorff, J. H. *Nano Lett.* **2005**, *5*, 429.

10.1021/cm702088v CCC: $40.75
Published on Web 12/22/2007

Scheme 1. Schematic Diagram of Face-to-Face Wetting[a]

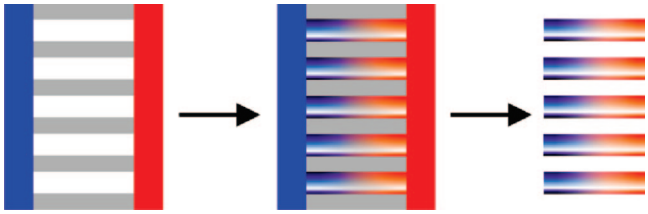

[a] Nanoporous disks with pores open at both ends are simultaneously exposed to different polymeric solutions. Both solutions infiltrate the pores from the opposite surfaces of the disks. As the solvents evaporate, the polymers solidify and gradient tubes are conserved. Optionally, they can be released by selectively etching the template disks. The method can also be adapted to the processing of polymeric melts.

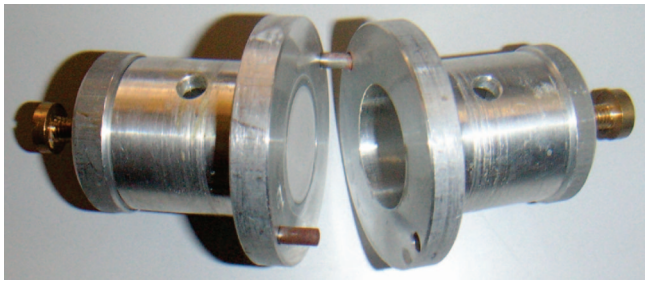

Figure 1. Experimental setup used for face-to-face wetting with solutions. The template disk is mounted in between two compartments. Polymeric solutions can be simultaneously injected into the compartments through small openings in their walls.

Nanorods[23–26] and nanotubes[27,28] consisting of segments of different functional materials have emerged as a new class of advanced one-dimensional nanostructures. They may be used as nanobarcodes, and specific segments can be chemically functionalized. Therefore, they are of tremendous interest for applications in the fields of nanobiosensors and nanoelectronics. Multisegment nanotubes and nanorods have been predominantly prepared by means of electrochemical methods. Recently, we have reported the fabrication of segmented tube/rod hybrid nanofibers by bidirectional template wetting.[29] In this procedure, pore segments with a specific length were partially filled by a slow and time-consuming capillary wetting step with a block copolymer. Subsequently, the templates were wetted from the reverse side under conditions where precursor wetting occurred.

Here, we report a simple, complementary approach for the fabrication of gradient nanotubes and segmented nanotubes referred to as face-to-face wetting that involves the rapid, simultaneous infiltration of different polymeric liquids from the opposite surfaces of a porous template. The electronic, optical, mechanical, and chemical properties of the nanostructures thus obtained potentially vary in an adjustable manner along their long axes, as required for a broad range of potential applications. For example, nanofibers with a gradient of their mechanical properties along their long axes may be used as building blocks for bioinspired adhesive structures. Face-to-face template wetting enables the integration of various functional materials, such as tailor-made organic compounds and polymers, into segmented or gradient nanotubes and nanorods. For face-to-face wetting simultaneously starting from the opposite surfaces of a porous template, any combination of polymeric materials that can be processed either as a melt or a solution can be used. As discussed below, face-to-face wetting with polymeric solutions may yield gradient nanotubes. The composition of their walls changes along the nanotubes. Moreover, our preliminary results suggest that the composition profile can be customized by controlling the compatibility of the infiltrated species. In contrast to face-to-face wetting with solutions, face-to-face wetting with melts leads to the filling of pore segments with the pure components so that a sharp interface forms between the segments of the formed nanostructures composed of different constituents.

Experimental Section

Chemicals. 4-Chloro-styrene (Acros) and 4-bromo-styrene (Acros) were dried over CaH_2 and purified by distillation. CH_2Cl_2 (BASF), MeOH (BASF) and 1,1,4,7,7-pentamethyldiethylenetriamine (Acros) were distilled before use. Hydrochloric acid (Merck), KOH (Merck) and CuBr (Acros) were used as received. Benzyl bromide (Merck) was dried with Na_2SO_4 and distilled. PVC (Vestolith; $M_n = 47\,800$ g/mol; $M_w = 92\,920$ g/mol; $M_w/M_n = 1.94$; $T_g = 79.5$ °C), fluorescent polymer PMMA/9-cinylanthracen (10%)-copolymer ($M_w = 27\,334$, $M_n = 17\,048$, University Marburg), PMMA (Polymer-Standard-Service PSS, $M_W = 120\,000$, and $M_w = 23\,300$, $M_n = 23\,000$) were used as received. Porous alumina membranes (Anodisk 25) were obtained from Whatman and used as received.

General Synthesis of PBrS and PClS. Atom transfer radical polymerization (ATRP)[30–33] was adapted to synthesize PClS and PBrS with high molecular weights on the order of 150.000 g/mol and low polydispersities. The polymerizations were carried out under argon in predried Schlenk tubes under ATRP reaction conditions. The reaction mixtures containing either 11 g (79.4 mmol) of 4-chlorostyrene or 14 g (76.5 mmol) of 4-bromostyrene, as well as 30 mg (0.18 mmol) of benzylbromide, 28.4 mg (0.2 mmol) of CuBr, and 35 mg (0.2 mmol) of *N*,*N*,*N*′,*N*″,*N*″-pentamethylenediethylenetriamine were degassed by three freeze–pump–thaw cycles, placed in a preheated oil bath at 125 °C for 72 h, and reacted at 125 °C. The reaction mixture was cooled to room temperature, dissolved in 320 mL of CH_2Cl_2 and precipitated into 1 L of methanol. Purification of the polymers was done by reprecipitation from CH_2Cl_2/methanol and drying at 50 °C in a high vacuum until the weight was constant. The molecular weights of the polymers were determined by size-exclusion chromatography using a Knauer HPLC 64 pump with PSS SDV linear 10 μm column

(21) Göring, P.; Pippel, E.; Hofmeister, H.; Wehrspohn, R. B.; Steinhart, M.; Gösele, U. *Nano Lett.* **2004**, *4*, 1121.
(22) Steinhart, M.; Zimmermann, S.; Schaper, A. K.; Ogawa, T.; Tsuji, M.; Gösele, U.; Weder, C.; Wendorff, J. H. *Adv. Funct. Mater.* **2005**, *15*, 1656.
(23) Nicewarner-Peña, S. R.; Griffith Freeman, R.; Reiss, B. D.; He, L.; Peña, D. J.; Walton, I. D.; Cromer, R.; Keating, C. D.; Natan, M. J. *Science* **2001**, *294*, 137.
(24) Salem, K.; Searson, P. C.; Leong, K. W. *Nat. Mater.* **2003**, *2*, 668.
(25) Park, S.; Lim, J.-H.; Chung, S.-W.; Mirkin, C. A. *Science* **2004**, *303*, 348.
(26) Hurst, S. J.; Payne, E. K.; Qin, L.; Mirkin, C. A. *Angew. Chem., Int. Ed.* **2006**, *45*, 2672.
(27) Sander, M. S.; Gao, H. *J. Am. Chem. Soc.* **2005**, *127*, 12158.
(28) Lee, W.; Scholz, R.; Nielsch, K.; Gösele, U. *Angew. Chem.* **2005**, *117*, 6204.
(29) Kriha, O.; Zhao, L; Pippel, E.; Gösele, U.; Wehrspohn, R. B.; Wendorff, J. H.; Steinhart, M.; Greiner, A. *Adv. Funct. Mater.* **2007**, *17*, 1327.
(30) Wickel, H.; Agarwal, S.; Greiner, A. *Macromolecules* **2003**, *36*, 2397.
(31) Wang, J. S.; Matyjaszewski, K. *Macromolecules* **1995**, *28*, 7901.
(32) Matyjaszewsky, K.; Xia, J. *Chem. Rev.* **2001**, *101*, 2921.
(33) Patten, T. E.; Matyjaszewski, K. *Adv. Mater.* **1998**, *10*, 901.

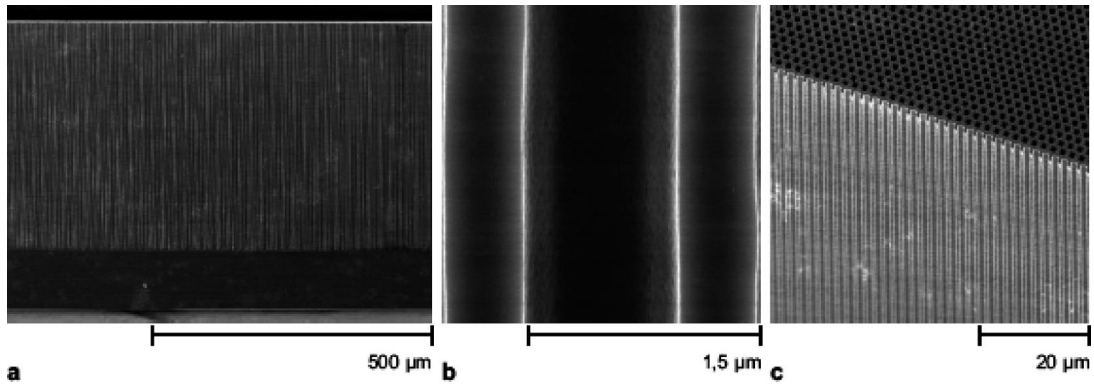

Figure 2. Scanning electron microscopy images of macroporous silicon with a pore diameter of 1 μm. (a) Cross-sectional view of macroporous silicon with a pore depth of 420 μm; (b) single pore; (c) edge of a macroporous silicon template.

equipped with a Knauer UV-detector. THF was used as eluent at 20 °C at a flow rate of 0.8 mL/min. Both IR and NMR data are in accordance with earlier works,[34,35] and the results of elemental analysis are in good accordance with the theoretical values.

Preparation of Nanotubes and Microtubes. To generate a compositional gradient in the longitudinal direction, melts or solutions containing different polymers were simultaneously exposed to the opposite surfaces of templates having pores open at both ends (Scheme 1). For face-to-face wetting with polymeric solutions, we used commercially available nanoporous alumina membranes (Whatman Anodisk; nominal pore diameter, 200 nm; pore depth, 60 μm) and the experimental setup shown in Figure 1, which consisted of two compartments. The template disks were placed between these two compartments, into which the polymeric solutions were simultaneously injected with syringes. Two minutes after the injection, the alumina disks were rapidly removed from the solutions and dried under ambient conditions.

For face-to-face wetting with polymeric melts, macroporous silicon[5–7] exhibiting a hexagonal pore lattice with an interpore distance of 1.5 μm and a pore diameters of about 1μm (Figure 2) was used as a template in order to prepare microtubes eligible for probing with a fluorescence microscope. The depth of the membrane pores was adjusted to values between 200 and 400 μm. Face-to-face melt wetting was carried out using a modified waffle iron. Both hot plates could be addressed individually by a computer-operated temperature controller. The macroporous silicon was placed in a specifically designed copper holder equipped with a poly(tetrafluoroethylene) sealing to minimize heat transfer between the two hot plates.

Characterization. For scanning electron microscopy (SEM) and EDXA (energy-dispersive X-ray analysis) measurements, the nanotubes were released by etching the templates with KOH. The base was removed by several centrifuging steps. A few droplets of a neutral, aqueous suspension of the nanotubes were dropped on aluminum sample holders, dried at ambient conditions, and coated with carbon. The EDXA measurements were performed using a CamScan CS 4 DV (Cambridge Scanning Company) equipped with a D-4649 detector (ThermoNoran) at accelerating voltages ranging from 15 to 20 kV. The SEM micrographs of uncoated samples were taken with a JEOL JSM 7401-F operated at 1 kV.

The optical characterization was made in transmission using an Olympus microscope (Coover 018) at 100× magnification. For the fluorescence microscopy, the samples were excited using an UV laser at 375 nm in reflection mode.

(34) Königsberg, I.; Jagur-Grodzinski, J. *J. Polym. Sci., Part A: Polym. Chem.* **1983**, *21*, 2649.
(35) Rincón Guerrero, A. *Polym. Bull.* **1995**, *35*, 143.

Scheme 2. Chemical Structures of the Model Polymers Used for Face-to-Face Wetting: (a) PClS, (b)PBrS, (c)PVC

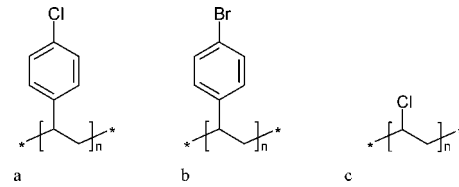

Results and Discussion

We applied two different methods for face-to-face wetting: solution wetting and melt wetting. Solution wetting was carried out by simultaneously infiltrating two polymeric solutions from the opposite surfaces of the templates at room temperature. In the case of melt wetting, two polymers were simultaneously infiltrated from the opposite surfaces of the templates at a temperature slightly above the melting point. In the following, we compare both methods and discuss the differences and possible mechanisms.

As model components for the investigation of room-temperature face-to-face wetting with polymeric solutions we selected poly(4-chlorostyrene) (PClS), poly(4-bromostyrene) (PBrS), and poly(vinylchloride) (PVC) (Scheme 2). The halogen atoms attached to each repeat unit are atomic labels that allow analyzing differences in composition by spatially resolved EDXA. It is expected that the compatibility of the structurally similar polymers PClS and PBrS is considerably higher than that of PVC and PBrS. Therefore, we compared the spatial distribution of Br and Cl within the walls of both PVC/PBrS and PClS/PBrS composite nanotubes.

To fabricate PVC/PBrS gradient nanotubes, we simultaneously wetted nanoporous alumina membranes (Whatman Anodisk) with a mean pore diameter of 200 nm with 5 wt % solutions of PVC in tetrahydrofuran (THF) and PBrS in dichloromethane (CH_2Cl_2). Figure 3a shows a SEM image of an array of PVC/PBrS gradient nanotubes that were released by etching the template with aqueous KOH. The tubular nature of the PVC/PBrS nanostructures is obvious from Figure 3b, where some tube openings are seen. The presence of a composition gradient was evidenced by EDXA. We selected the L_α peak of Br at 1.480 keV, and the K_α peak of Cl at 2.622 keV to probe the presence of these elements within the walls of the nanotubes. Figure 3c shows the intensity profile of the K_α peak of Cl, recorded by a line scan along a path parallel to the long axes of the nanotubes

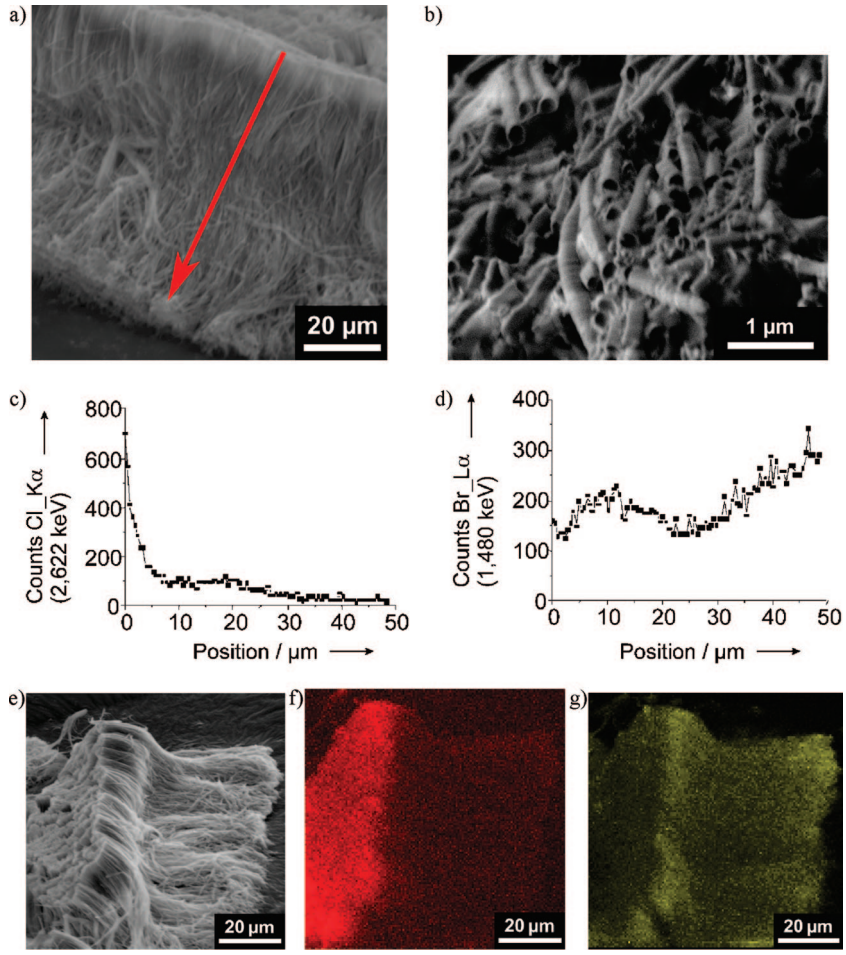

Figure 3. PVC/PBrS gradient nanotubes. (a) SEM picture of an array of nanotubes; (b) detail showing tube openings; (c) corresponding intensity profile for the K_α peak of Cl, and (d) for the L_α peak of Br along a path parallel to the long axes of the tubes, as indicated by the red arrow in (a). (e) Conventional SEM picture of an array, (f) corresponding two-dimensional mapping of the intensity of the K_α peak of Cl, and (g) of the L_α peak of Br. The color intensity encodes the peak intensity.

as indicated by the red arrow in Figure 3a. The corresponding curve for the L_α peak of Br is seen in Figure 3d. The scan started at the edge of the nanotube array originally located at the template surface exposed to the PVC solution (position = 0 μm) and ended at the edge of the nanotube array originally located at the template surface exposed to the PBrS solution (position = 50 μm). The path length of the line scan is smaller than the length of the tubes because the cross-section of the array is bent. The tube segments initially located in the proximity of the template surface exposed to the PVC solution show a pronounced enrichment of Cl. At a distance of 5 μm from the edge, the concentration of Cl steeply decreases. Br is present over the entire length of the tubes, but the intensity of the Br signal increases as the distance to the edge of the nanotube array initially located at the template surface exposed to the PBrS solution decreases. This was confirmed by the investigation of a cross-section at a different location in the gradient nanotube array: Figure 3e shows the corresponding SEM image, Figure 3f a two-dimensional mapping of the intensity of the Cl signal (red), and Figure 3g a two-dimensional mapping of the intensity of the Br signal (yellow).

The EDXA experiments confirm that the PVC/PBrS nanotubes, which consist of chemically different components (Scheme 2), are characterized by a pronounced longitudinal composition gradient. In a further set of experiments, we investigated nanotubes composed of PBrS and PClS. Apart from the halogen atom on the aromatic core, these two polymers consist of structural identical repeat units. Consequently, the compatibility of the binary system PClS/PBrS should be higher than that of the binary system PVC/PBrS. PClS/PBrS nanotubes were fabricated using 5 wt % solutions of the polymers in CH_2Cl_2, but otherwise under the same conditions than the PVC/PBrS gradient nanotubes. A cross-sectional view on an array of released PClS/PBrS nanotubes is seen in Figure 4a. The intensity profile of the K_α peak of Cl, recorded by a line scan along a path parallel to the long axes of the nanotubes as indicated by the red arrow in Figure 4a, is shown in Figure 4b. The corresponding curve for the L_α peak of Br is shown in Figure 4c. The scan started at the edge of the nanotube array originally located at the template surface exposed to the PBrS solution (position = 0 μm) and ended at the edge of the nanotube array originally located at the template surface exposed to the PClS solution (position = 60 μm). Two-dimensional mappings of the EDXA intensities of the array seen in Figure 4d are shown in Figure 4e for the Cl signal (red) and in Figure 4f for the Br signal (yellow). As in case of the PVC/PBrS system, the PClS/

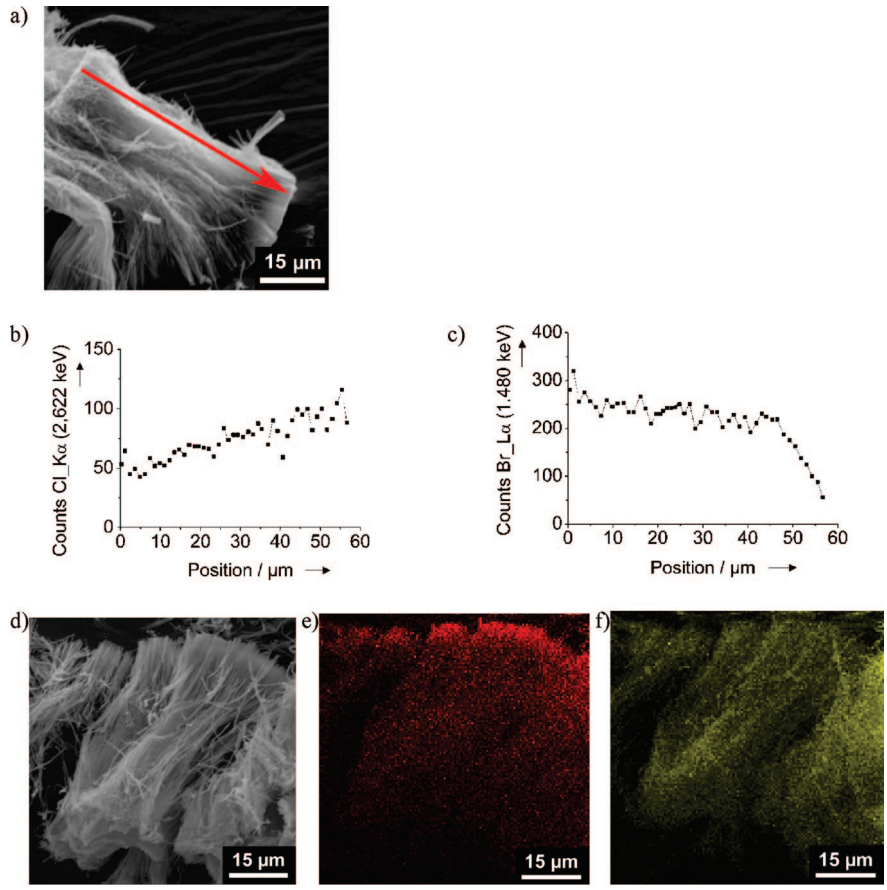

Figure 4. PClS/PBrS gradient nanotubes. (a) SEM picture of an array. (b) Corresponding intensity profile for the K_α peak of Cl and (c) for the L_α peak of Br along a path parallel to the long axes of the tubes, as indicated by the red arrow in (a). (d) Conventional SEM picture of an array, (e) corresponding two-dimensional mapping of the intensity of the K_α peak of Cl, and (f) of the L_α peak of Br. The color intensity encodes the peak intensity.

PBrS gradient nanotubes contain both chlorine and bromine. The relative concentration of both elements increases as the distance to the edge of the nanotube array originally located at the template surface exposed to the solution containing the correspondingly labeled polymer decreases. However, particularly the distribution of chlorine is much more homogeneous as compared to the PVC/PBrS gradient nanotubes. This finding might be attributed to a higher compatibility of the components.

In contrast to wetting with polymeric solutions, in face-to-face melt wetting experiments the same type of polymers was used in order to ensure that the melts located at both template surfaces move into the pores at a comparable rate. To distinguish between the polymers moving into the pores from the opposite sides of the templates, we synthesized a tailor-made polymer with a chromophore bonded to the polymer backbone by radical copolymerization of methylmethacrylate and anthracenoyl methacrylate (content about 0.2 mol %). Wetting experiments were carried out with a fluorescent (PMMA/9-vinylanthracen (10%)-copolymer) and a nonfluorescent polymer (PMMA) using macroporous silicon membranes with a thickness of 270 μm and a pore diameter of 1 μm as porous templates. Macroporous silicon was selected as a template system in order to prepare tubes with a well-defined shape large enough to be characterized by optical microscopy.

In the first series of experiments performed at an infiltration temperature of 180 °C, the nonfluorescent PMMA used had a significantly higher molecular weight (M_w = 120 000 g/mol) than the fluorescent PMMA/9-vinylanthracen (M_w = 27 334 g/mol, M_n = 17 048 g/mol). Along the tubes thus obtained, we observed uniform luminescence (Figure 5). This can be explained by the lower viscosity and therefore faster infiltration of PMMA/9-vinylanthracen as compared to the more viscous nonfluorescent PMMA, resulting in the formation of a wetting film on the pore walls exclusively consisting of PMMA/9-vinylanthracen.

To verify this hypothesis, we selected PMMA (M_w = 23300 g/mol, M_n = 23000 g/mol; obtained from Polymer Standard Service, Germany) with a molecular weight comparable to that of the PMMA/9-vinylanthracen. Face-to-face wetting at 180 °C and subsequent release of the tubes thus obtained yielded luminescent tube segments as well as nonluminescent tube segments (Figure 6). The nonluminescent tube segments were optically completely inactive except, in some cases, at the ends of the tube segments. In contrast, the luminescent tube segments predominantly show homogeneous luminescence along their entire length.

Apparently, the two molten polymeric components do not mix when they impinge on each other in the course of the wetting process. Therefore, the tubes preferentially break at

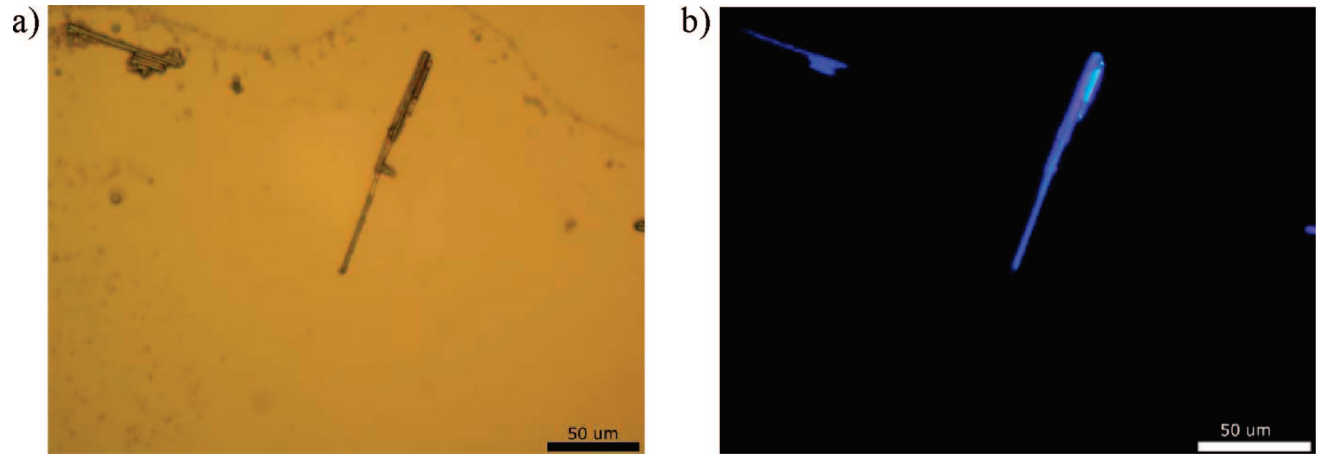

Figure 5. (a) Optical and (b) fluorescent microscopy images of PMMA/9-vinylanthracen tubes obtained by face-to-face melt wetting. The infiltration of the fluorescent PMMA/9-vinylanthracen melt occurs at a much higher rate than the infiltration of the second component PMMA with significantly higher molecular weight. All tubes are fluorescent over their entire length.

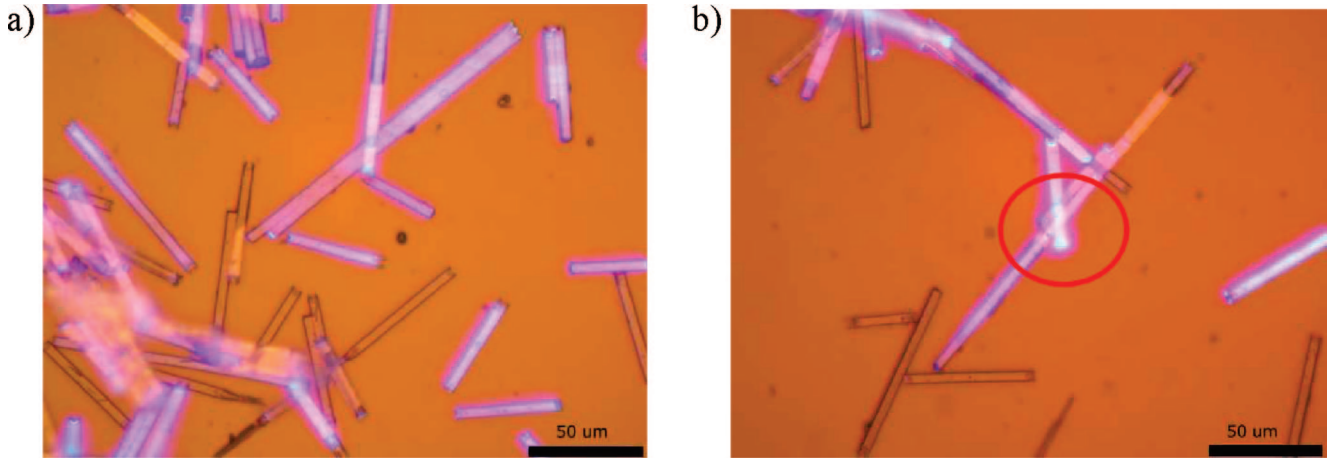

Figure 6. (a, b) Fluorescent microscopy images of nonfluorescent PMMA tube segments and fluorescent PMMA/9-vinylanthracen tube segments obtained by face-to-face melt infiltration of PMMA and PMMA/9-vinylanthracen having similar molecular weights. The red circle in (b) indicates the interface between a nonluminescent and a luminescent part of the tube.

the interface between the tube segments thus formed when exerted to mechanical stress in the course of their release. This finding indicates the presence of a sharp, well-defined interface between the two polymeric components. Polymers are commonly immiscible because the combinatorial entropy generated upon mixing, as compared to low-molecular-mass compounds, is negligible. This effect is well-known from polymer processing. Flow lines resulting from the merging of two different flow fronts in, for instance, injection molding tend to be weak because of a mismatch in chain orientations and conformations even for compatible systems. Therefore, face-to-face wetting using polymeric melts is complementary to face-to-face wetting using polymeric solutions. In the latter case, the solvents may act as compatibilizer between the polymeric components so that a real gradient zone forms.

Conclusion

We have developed a face-to-face wetting method that involves rapid, simultaneous wetting of porous templates from their opposite surfaces. The use of polymeric solutions yields nanotubes with a longitudinal composition gradient dependent on the compatibility of the components. Face-to-face wetting with polymer melts leads to segmented tubes consisting of segments separated by a sharp, well-defined interface. The method presented here can be easily extended, for example, for the fabrication of nanoparticle-containing polymer nanotubes with a longitudinal gradient in the nanoparticle content, and thus longitudinal gradients in functionality.

Acknowledgment. The authors thank the German Science Foundation (DFG) for funding in the framework of the priority program SPP 1165 (WE 2637/6 and STE 1127/6-2) and Dr. Paul Miclea for technical support.

Supporting Information Available: Elemental analysis and other characterization details (PDF). This material is available free of charge via the Internet at http://pubs.acs.org.

CM702088V